



Organotypic culture of bone-like structures using composite ceramic-fibrin scaffolds

Journal:	<i>Current Protocols</i>
Manuscript ID	CP-18-0228.R1
Wiley - Manuscript type:	Protocol
Date Submitted by the Author:	17-Dec-2018
Complete List of Authors:	Iordachescu, Alexandra; University of Birmingham, Chemical Engineering; University of Oxford, Botnar Research Centre Williams, Richard; University of Birmingham, Chemical Engineering Hulley, Philippa; University of Oxford, Botnar Research Centre Grover, Liam; University of Birmingham, Chemical Engineering
Keywords:	Bone, Organotypic Culture, Biomaterials, Self-organisation, Osteocytes
Abstract:	We have developed an organotypic culture system that allows the production of bone tissue features at the cm scale. A composite, calcium phosphate-strained fibrin gel system is able to organise itself in the presence of osteoblastic cells, creating basic hierarchical units as seen in vivo, and can be modified to produce a range of other tissues that require such directional structuring. Constructs evolve over time into multi-compositional structures containing a high mineral content and terminally differentiated, osteocyte-like cells. These tissues can be cultured over extended durations (exceeding 1 year) and are responsive to a variety of chemical and biological agents. The platform can reduce the number of animals used in experimentation by acting as an intermediate stage in which more personalised research conditions can be generated. We provide a thorough description of the protocol used to successfully culture and modify this system as well as guidance on compositional characterisation.

SCHOLARONE™
Manuscripts



Organotypic culture of bone-like structures using composite ceramic-fibrin scaffolds

Alexandra Iordachescu^{*1,2}, Richard L. Williams¹, Philippa A. Hulley^{2#}, Liam M. Grover^{1#}

¹School of Chemical Engineering, University of Birmingham, Edgbaston, Birmingham, UK, B15 2TT

²Botnar Research Centre, University of Oxford, Old Road, Headington, Oxford, UK, OX3 7LD

[#]contributed equally to this work.

^{*}Correspondence: A.Iordachescu@bham.ac.uk

Significance Statement

This protocol presents a method to produce mature bone-like tissue *in vitro* using geometrically-strained fibrin templates, supporting new cell matrix forming around ceramic holding points. These tissues develop longitudinally from the retention points, with cells using the ceramics to generate mature bone mineral together with newly secreted collagen. Further similarities to *in vivo* bone can be seen in the mineral:matrix ratio and the mature cell phenotype, osteocytic, which can be differentiated from an initial osteoblastic population. The platform can be used as a non-animal based research tool and represents a cost-effective way to evaluate promising drug formulations. It can be adapted for a multitude of cell phenotypes, encouraging aligned tissue formation and by fine-tuning an initial stem cell population.

ABSTRACT

We have developed an organotypic culture system that allows the production of bone tissue features at the cm scale. A composite, calcium phosphate-strained fibrin gel system is able to organise itself in the presence of osteoblastic cells, creating basic hierarchical units as seen *in vivo*, and can be modified to produce a range of other tissues that require such directional structuring. Constructs evolve over time into multi-compositional structures containing a high mineral content and terminally differentiated, osteocyte-like cells. These tissues can be cultured over extended durations (exceeding 1 year) and are responsive to a variety of chemical and biological agents. The platform can reduce the number of animals used in experimentation by acting as an intermediate stage in which more personalised research conditions can be generated. We provide a thorough description of the protocol used to successfully culture and modify this system as well as guidance on compositional characterisation.

Keywords: Bone, Organotypic Culture, Biomaterials, Self-Organisation, Osteocytes

INTRODUCTION

In vitro cell cultures are widely used as a first-stage method for assessing the behaviour of bone-building cells (osteoblasts and osteocytes) under physiological and pathological conditions. These cells can either originate from primary bone sources, being isolated through matrix digestion; expanded from bone fragments; or used from highly-proliferative populations (e.g. MC3T3-E1, 2T3, MLO-Y4) (Ghosh-Choudhury, Windle et al. 1996, Kato, Windle et al. 1997, Mizutani, Sugiyama et al. 2001, Sowa, Kaji et al. 2002, Zhao, Zhang et al. 2002). They are subsequently expanded on rigid, flat surfaces, where they can form a two-dimensional monolayer and produce osteoid and mineralisation nodules (Bellows, Aubin et al. 1986, Buttery, Bourne et al. 2001, Wang, Liu et al. 2006).

Whilst 2D cell culture is an excellent tool for reproducibility and standardisation, it cannot generate the bone architecture and cellular interactions found *in vivo*, as the cells are unable to assemble into hierarchical, three-dimensional structures, or without becoming hypoxic. Murine models can provide an environment of sufficient complexity to study these processes, however they require using large populations of animals for obtaining consistent results, and in most cases the systemic interactions make it difficult to isolate individual factors in early stage bone tissue formation (Kaplan, Shore et al. 2005, Kan and Kessler 2011, Anthonissen, Ossendorf et al. 2016). Therefore, three-dimensional models that are more advanced structurally compared to monolayer populations but that can address the

1
2
3
4
5
6
7
8
9
10
11
12
13
14
15
16
17
18
19
20
21
22
23
24
25
26
27
28
29
30
31
32
33
34
35
36
37
38
39
40
41
42
43
44
45
46
47
48
49
50
51
52
53
54
55
56
57
58
59
60

limitations with multi-factorial *in vivo* rodent models offer the possibility to investigate primary cells over further stages of development. Moreover, when used with primary patient-derived cells, they can help in studying the diversity and heterogeneity of aberrant tissue formations and in developing personalised medical therapies (Mitra, Mishra et al. 2013, Neves, Rodrigues et al. 2016, Kodack, Farago et al. 2017).

Many biomaterials and methods have been developed over the years for producing physiologically relevant bone-like cultures *in vitro* (Edmondson, Broglie et al. 2014, Bouet, Cruel et al. 2015). These involve applying stem cells or osteoblasts to a variety of scaffolds including natural or synthetic polymers such as hydrogels or elastomers (Liu, Zeng et al. 2017). Other materials include bioactive ceramics such as calcium phosphates (Wang, Zhao et al. 2014) and bioactive glasses (Rahaman, Day et al. 2011).

Composite systems containing both ceramics and polymers have been used to increase the mechanical properties of the scaffolds and to simulate the biochemical composition of bone (Wahl and Czernuszka 2006, Chesnutt, Viano et al. 2009, Moreau, Weir et al. 2009, Šupová 2009, Maas, Guo et al. 2011, Thein-Han, Liu et al. 2012, Wang, Bongio et al. 2014).

Some of the hydrogels used in these studies include gelatin, chitosan, alginate, hyaluronic acid, polyethylene glycol, collagen I and fibrin, each with significant advantages and disadvantages (Lee and Mooney 2001, Perka, Stern et al. 2003, Chesnutt, Viano et al. 2009, Wang, Bongio et al. 2014). For bone tissue generation, collagen type I gels are the most popular choice due to its chemical and structural similarity to the osteoid of bone (Kikuchi, Itoh et al. 2001, Wahl and Czernuszka 2006, Moreau, Weir et al. 2009, Matthews, Naot et al. 2014). However, the chemistry of these scaffolds makes it difficult to study early bone formation, as the new collagen produced by embedded cells is difficult to separate from the collagen present in the original matrix.

Fibrin hydrogels have been widely used for many years as alternatives to collagen gels (Eyrich, Brandl et al. 2007, Eyrich, Göpferich et al. 2007) as they are chemically similar to blood clots, the first scaffold encountered by many types of cells during tissue trauma, healing and repair (Janmey, Winer et al. 2009). They exhibit a high bioactivity and are able to bind cells, growth factors, nutrients and metabolites, thus being excellent substrates for stem cell differentiation (Lee and Mooney 2001, Drury and Mooney 2003). Whilst they have a limited mechanical strength (Lee and Mooney 2001), these hydrogels are degradable in the presence of cells, which means that, as seen during wound healing, they can be replaced over time with endogenous cell-secreted collagenous matrix that can ultimately become mineralised and mimic the composition and geometry of *in vivo* bone tissue. Fibrin gels can be easily assembled by

polymerisation of fibrinogen in the presence of thrombin and can even be produced from the patient's own blood components (Lee, Kwan et al. 2008, Ahmed, Ringuette et al. 2015), making them ideal for developing personalised tissues for transplantation. In addition, their degradation rate can be matched to that of new tissue formation by adding inhibitors of proteolytic enzymes, such as aprotinin (Ye, Zund et al. 2000).

Whilst these cell-scaffold constructs can simulate the biochemical composition of bone tissue, to date, there are no *in vitro* 3D cell culture systems that are able to robustly simulate the micro-architecture of bone tissue (Weinbaum, Cowin et al. 1994, Boukhechba, Balaguer et al. 2009, Vazquez, Evans et al. 2014). Both trabecular and lamellar bone, whilst being morphologically and functionally different at the tissue level, at the micro-scale have a similar structural organisation where mineralised collagen fibres are aligned with their respective mechanical axis (Reznikov, Chase et al. 2015).

We have recently developed a biomechanically-strained fibrin culture system which can self-structure upon seeding with primary cells and develops internal tensile forces that align the cells and matrix longitudinally, allowing an organised temporal evolution of bone mineral, cells and microstructure over significant periods of time (over 1 year of culture) (Iordachescu, Amin et al. 2018).

This system has been extensively tested using populations of osteoprogenitor cells extracted from the periosteum of rat femoral bones, which are key players during fracture repair and are able to use the formed blood clot as a template to generate new bone (Einhorn and Gerstenfeld 2015). Furthermore, they have been shown to generate bone when implanted in muscle (Ueno, Kagawa et al. 2003), and therefore may be central to pathological conditions in which soft-tissues develop ossifications. Following isolation, periosteal cells are seeded into polymerised fibrin gels, representative of the structure and biochemistry of the callus formed early in bone fracture healing or the early-wound microenvironment in pathological ossification.

To encourage matrix organisation, the callus-like fibrin gel is manipulated using two calcium phosphate anchors composed of a mixture of brushite ($\text{CaHPO}_4 \cdot 2\text{H}_2\text{O}$) and β -TCP ($\text{Ca}_3(\text{PO}_4)_2$), inserted at the extremities of the culture dish. Cells contract the fibrin around these two retention points over the first culture week, creating tensile forces that lead to cellular and matrix alignment. The ceramic anchors also provide a source of calcium and phosphate ions that locally-trigger the ossification process. Over time, these constructs evolve from flat gels into cylindrical structures that are chemically heterogeneous, show a degree of organisation and are clinically-relevant. We have also shown that they are a rich source of physiologically-relevant nanostructures (Iordachescu, Hulley et al. 2018).

This model can be adapted for applications in a wide range of areas, from toxicology to regenerative medicine.

It also provides users with the platform to further develop it into a tool that may facilitate clinical translation of their own technologies and supports the current industrial climate for adoption of non-animal based screening and testing platforms.

From an industrial perspective, the model potentially provides a more cost effective and lower maintenance tool for selecting promising drug formulations.

The following protocol documents the methodology for creating the bone culture model described above in response to limitations with existing *in vivo* and *in vitro* models and captures know-how that will enable other users to modify the culture system with alternative cell populations. It also discusses the appropriate selection of physicochemical characterisation methods based on the biologically/structurally-relevant feature of the tissue the users wish to evaluate. This information has important implications on cost efficient use of the model and sample preparation to maximise the quality of the measurements.

BASIC PROTOCOL 1

PRODUCTION OF BONE CONSTRUCTS

The following protocol thoroughly describes the steps required for production and culture of bone tissue-like constructs. These constructs can be used as an additional, non-animal based platform for investigating normal and aberrant bone formation and for evaluating promising drug formulations. Steps 1-3 of this protocol detail the assembly process and specific details for successfully building the different components of this system. Step 4 provides a description of the procedure for isolating periosteal cells, essential for initiating ossification in these constructs. Steps 5-9 describe the process of generating the fibrin scaffolds and cell embedding as well as maintenance of constructs. These steps are followed by detailed outcomes on the self-organising process and guidelines for monitoring and chemically evaluating ossification.

Materials

6-Aminohexanoic Acid (Powder, ≥ 98.5%, Sigma - Aldrich, St. Louis, Missouri, USA, Cat. No. 07260) (see recipe)

Aprotinin, Bovine Lung, Lypophilized powder, Ultrapure, 10 mg (Affymetrix Inc., Cleveland, Ohio, USA, Cat. No. 9087-70-1, Stock No. 11388) (see recipe)

L-ascorbic acid 2-phosphate sesquimagnesium salt hydrate (Sigma - Aldrich, St. Louis, Missouri, USA, Cat. No. 8960) (see recipe)

Sodium β -Glycerophosphate pentahydrate $[(\text{HOCH}_2)_2\text{CHOPO}(\text{ONa})_2 \cdot 5\text{H}_2\text{O}]$ commercially available e.g. Alfa Aesar, Heysham, England, Cat. No. L03425) (see recipe)

β – TCP Powder $[\text{Ca}_3(\text{PO}_4)_2]$, < 125 μm particle size (Commercially available. The powder used in our studies is manufactured by reactive sintering of a powder containign CaHPO_4 (Mallinckrodt – Baker, Germany) and CaCO_3 (Merck, Germany), with a theoretical calcium to phosphate molar ratio of 1.5. The powder mixture is suspended in absolute ethanol and mixed for 12 hours. The suspension then undergoes filtration and the resulting cake is heated in an alumina crucible to 1400° C for 12 hours and 1000° C for 6 hours before quenching in a dissicator in ambient conditions. The resulting sinter cake is then crushed using a pestle and mortar and is passed through a 125 μm sieve)

Bovine Serum Albumin (Sigma - Aldrich, St. Louis, Missouri, USA, Cat. No. A8806)

Collagenase (Gibco®, Life Technologies, Grand Island, New York, USA, Cat. No. 17018 - 029) (see recipe)

Collagenase Type II (Gibco®, Life Technologies, Grand Island, New York, USA, Cat. No. 17101 - 015) (see recipe)

Dispase I (Gibco®, Life Technologies, Grand Island, New York, USA, Cat. No. 17105 - 041) (see recipe)

Dexamethasone ($\text{C}_{22}\text{H}_{29}\text{FO}_5$, Powder, suitable for cell culture, $\geq 97\%$, e.g. Sigma - Aldrich, St. Louis, Missouri, USA, Cat. No. D4902) (see recipe)

Dulbecco's Modified Eagle Medium (High Glucose - 4.5 g/L, Gibco®, Life Technologies, Grand Island, New York, USA, Cat. No. 41966) (see recipe)

Dulbecco's Modified Eagle Medium (Low Glucose - 1 g/L, Gibco®, Life Technologies, Grand Island, New York, USA, Cat. No. 31885) (see recipe)

F12K Nutrient Mixture (1X) with Kaighn's Modification (Gibco®, Life Technologies, Grand Island, New York, USA, Cat. No. 21127-022)

Fetal Bovine Serum (Sterile filtered, suitable for cell culture, ≤ 10 EU/ml endotoxin, ≤ 25 mg/dL haemoglobin e.g. Sigma - Aldrich, St. Louis, Missouri, USA, Cat. No. F7524)

Fibrinogen, Bovine-Derived (≥75% of protein is clottable, Sigma - Aldrich, St. Louis, Missouri, USA, Cat. No. F8630)

(see recipe)

Orthophosphoric Acid (≥ 85% wt.% H₃PO₄, e.g. Sigma - Aldrich, St. Louis, Missouri, USA, Cat. No. 452289)

Penicillin-Streptomycin Solution (10,000 U Penicillin, 10 mg/ml Streptomycin, stabilised, sterile-filtered, suitable for cell culture e.g. Sigma - Aldrich, St. Louis, Missouri, USA, Cat. No. P4333)

Phosphate Buffered Saline Solution (pH = 7.4; Gibco®, Life Technologies, Grand Island, New York, USA, Cat. No.10010023)

Sylgard 184 Silicone Elastomer Kit (Base and Curing Agent, Dow Corning Corporation, Midland, Michigan, USA)

Thrombin Powder, Bovine-Derived, 1KU (EMD Millipore Corp., Billerica, MA, USA, Cat. No. 605157) (see recipe)

Trypan Blue Stain 0.4% (Life Technologies Corporation, Eugene, Oregon, USA, Cat. No. T10282)

TrypLE Select enzyme (pH 7.0-7.4, 1X, Gibco®, Life Technologies, Grand Island, New York, USA, Cat. No. 12563029)

Equipment

3D Modelling Software (e.g. SolidWorks, Dassault Systèmes, Vélizy-Villacoublay, France)

3D Printer and 3D Printing Filament (e.g. fused deposition modeling printer and corresponding thermoplastic feedstock)

Cell Culture Flasks (Culture Treated, T75, T175)

Cell Strainers, Nylon, 70 µm pore size, (Falcon, Corning Inc., Corning, New York, USA, Cat. No. 352350)

Countess™ Automated Cell Counter (or Equivalent) (Invitrogen™, Eugene, Oregon, USA)

Countess® Cell Counting Chamber Slides (or Equivalent) (Invitrogen™ Molecular Probes™, Eugene, Oregon, USA, Cat. No. C10228)

Culture plates (6-well, Clear, Sterile)

Elastomeric Impression Material (Silicone rubber e.g. Dow Corning 734, Dow Corning Corporation, Midland, Michigan, USA)

100% Ethanol (Molecular Grade Certified)

37°C, 5% CO₂ Humidity Incubator

Insect Pins, Stainless Steel (0.20 mm ø, Austerlitz Insect Pins®, Cat. No. 26002 - 20)

Laminar Flow Cabinet**Microscope** (Brightfield, Inverted)**Pipette Tips** (10 µl, 20 µl, 200 µl, 1000 µl, Sterile, DNase/RNase certified)**Pipettes** (0.5 µl – 1000 µl)**Polystyrene 48-well plate** (Clear, Sterile)**Scalpels** (Disposable, Sterile, DNase/RNase certified)**Scalpels** (Metallic, Sterilised)**Scissors** (Metallic, Sterilised)**Serological Pipettes** (10 ml – 25 ml, Sterile)**Spatulas** (Disposable, Sterile, DNase/RNase certified)**Steriflip-GP Sterile Centrifuge Tube Top Filter Unit** (50 ml, 0.22 µm Pore Size, Sterile, Merck – Millipore, Burlington, Massachusetts, United States Cat. No. SCGP00525)**Syringe Filters, 0.22 µm Pore Size, Sterile** (e.g. EMD Millipore™ Millex™-GP Sterile Syringe Filters with PES Membrane, Merck – Millipore, Burlington, Massachusetts, United States Cat. No. SLGP033RS)**Syringes** (Disposable, Sterile, 1ml - 10 ml)**Tubes** (Disposable, 5, 15, 50 ml, Sterile)**Vibrating Platform** (Generic Dental Laboratory Vibrator)**Virkon Disinfectant Powder****37°C Water Bath** (Clean, Sterile)**Weighing Boats** (Sterile, 5 – 7ml volume)**Wire Cutter** (Small)**STRATEGIC PLANNING****Aseptic technique and contamination prevention**

1. Conduct cell work in sterile conditions inside the laminar flow cabinets.
2. Sterilise cabinets using UV light overnight or for 12 hours if lamp is included in the design of the machine.
3. Prepare 70% Ethanol (EtOH) using sterile H₂O and 100% EtOH of molecular grade certification.

4. Prepare Virkon solution for disinfection by dissolving Virkon powder in ultrapure H₂O to a concentration of 1% (or use an equivalent, laboratory compatible disinfectant).
5. Spray the working surface with the Virkon solution to remove potential contaminants.
6. Wipe the excess liquid with sterile paper wipes.
7. Spray the working surface with 70% EtOH.
8. Allow the EtOH to evaporate for 10-15 minutes.
9. Sterilise dissection tools, pipettes and other metallic tools using overnight or 12 hour exposure to UV light in the laminar flow hood (if available).
10. Immerse the tools in 70% EtOH for 30 minutes on the day of use inside the flow hood cabinet.
11. Remove tools from 70% EtOH and allow to dry on the sterile surface for 15-30 minutes.
12. Use pipette tips, 1.5, 15 and 50 ml tubes that are sterile and DNase and RNase certified (optional).
13. Use culture-treated flasks for growing cell cultures.

Design and production of template moulds for anchor generation

1. Use a 3D modelling software to design a rectangular frame containing 20 or more trapezoidal geometric shapes measuring approximately 4 mm x 2 mm x 4 mm height (Figure 1a-b).
2. Use a 3D printer to produce plastic casting frames (Figure 1a-b).
3. Fill the hardened plastic frames with an elastomeric impression material of your choice (e.g. dental impression material)(Figure 1c).
4. Allow the material to set for at least 72 hours.
5. Remove the silicone mould from the plastic template.
6. Use the trapezoidal wells to insert the calcium phosphate paste (illustrated in Figure 1d and described in the next sections).
7. Prepare several moulds to enable the production of a stock of ceramic anchors in advance (Figure 1e).

Protocol steps

1. Production of the mineral component

Critical Parameter

To be performed 2 weeks before the commencement of the study.

- a. Calculate the number of anchors adequate for the number of constructs (2 per construct).
- b. Place a large weighing boat (minimum 5 ml capacity) on top of a vibrating platform.
- c. Add 2.5 g of β -TCP powder (<125 μ m particle size).
- d. Add 1 ml of Orthophosphoric Acid (3.5 M) to the boat to generate a paste composed of a mixture of brushite and β -TCP.
- e. Quickly mix for 1-2 seconds using a sterile spatula to ensure the setting is even.
- f. Place the cooled moulds on top of the vibrating platform.

- g. Pour the liquid mixture into the individual, pre-shaped wells of moulds on top of the vibrating platform to encourage uniform setting inside the shapes.
- h. Use the sterile spatula to break any air bubbles and pack the cement into the moulds.
- i. Using tweezers, carefully insert 1.4 cm stainless steel insect pins (0.20 mm diameter) into the individual wells of the moulds before the mixtures advances into a solid state.
- j. Allow the mixtures containing the pins to fully harden for 3-4 hours (Figure 1d).
- k. Remove the individual anchors from their moulds and store in a sterile culture dish until use (Figure 1 e).
- l. The final anchors have a trapezoidal shape and measure approximately 2 mm x 4 mm x 4mm in height (Figure 1e).

2. Coating of culture plates

Critical Parameter

To be performed 2 weeks before the commencement of the study.

See Figure 2 for a schematic representation of the steps described here.

- a. Use the colourless Sylgard184 polydimethylsiloxane elastomer and associated curing agent provided by the supplier.
- b. Prepare the base of the wells by mixing the Sylgard base to a curing agent at a 10:1 ratio inside a large weighing boat (up to 10 ml capacity), proceeding quickly.
- c. Aspirate and pour 1.5 ml of the silicone elastomer base into each well using a standard 10 ml syringe to coat them uniformly.
- d. Place the plates on a flat surface and allow them to dry at room temperature for 7 days to allow polymerization.

3. Assembly of the mineral 'backbone'

Critical Parameter

To be performed 2 weeks before the commencement of the study.

See Figure 2 for a schematic representation of the steps described here.

- a. Measure a distance of 1.5 cm in the centre of the wells using a standard ruler.
- b. Mark the desired insertion points of the anchors on the plastic back of the 6-well plate using a permanent marker.
- c. Cut the anchor pins to length using a small wire cutter allowing enough length so that the bottom surface of the anchors is in contact with the elastomer coating after insertion.
- d. Attach two anchors per 35 mm culture well to the hardened silicone base using their pins, ensuring that the distance reaches from the inner edge of one anchor to the other.
- e. *Optional* – plates without anchors can be used as contraction controls.
- f. Sterilise plates the day before the commencement of the experiment by spraying with 70% EtOH prepared using molecular grade water, inside a running, clean flow hood. Spray both the outside and the inside of the plates and allow to dry in the hood for 3-4 hours.

- g. Turn the flow off and proceed to sterilising the plates further using UV light (if available in the flow hood). Position the plates at an angle using their lids in a way that allows UV light to reach the wells.
- h. Lock the flow cabinet door.

4. Isolation and culture of primary femoral cells

- a. Use a minimum of 3 euthanised donor rats (Wistar, 3 weeks old, 50-70 grams weight) for extracting cells in each study.
- b. Carefully remove the surrounding muscular and connective tissue from excised femurs using scissors and scalpels.
- c. Place femurs in phosphate buffered saline solution.
- d. Place each bone inside a 15 ml tube containing the enzymatic digestion cocktail.
- e. Incubate the bones with this solution at 37°C for 1 hour inside a 5% CO₂ atmosphere incubator.
- f. Following incubation, shake the tubes rigorously for 30 seconds to detach the remaining cells and release them into the solution.
- g. Pass the solution through 70 µm pore filters placed on top of 50 ml tubes in order to isolate the cells from the remaining tissue debris.
- h. To recover the periosteal cells from solution, centrifuge the tubes at 1400 rpm for 6 min (21°C).
- i. Carefully remove the supernatant using a 25 ml serological pipette.

Critical Parameter

Great care must be taken to prevent aspiration of the cells, which have peletted at the bottom of the tube.

- j. Resuspend the cell pellet in 10 ml of D20 growth medium, which is used at a higher concentration to encourage cellular attachment to the culture flasks.
- k. Pipette up and down until the solution looks homogenous and no cellular clusters can be observed floating.
- l. Count the number of cells isolated per ml using an automated cell counter. Refer to your manufacturer's guidelines for instructions.

Critical Parameter

The use of an automated counter is recommended at all steps for consistency and speeding up the process in order to maximise the viability of isolated cells.

- m. Add approximately 1 million cells suspended in 10 ml D20 to 175 cm² culture flasks containing additional 25 ml D20 medium (or adjust the volumes accordingly to 35 ml).
- n. Place the culture flasks inside a 37°C, 5% CO₂, humidity-controlled incubator containing copper sulphate water (1 g/L) to prevent fungal contamination.
- o. Allow the cells to attach and proliferate for 2-3 days without replacing the medium.
- p. Observe the cells using an inverted microscope daily.
- q. Once the cells have reached a level of 70% confluency they are ready to be seeded into constructs.

5. Development of fibrin scaffolds

See Figure 2 for a schematic representation of the steps described here.

- a. Fibrin scaffolds are generated on top of the mineral backbone structure by mixing the normal plasma components fibrinogen and thrombin (which will be resuspended in a thrombin solution).
- b. Calculate the amount of thrombin solution and fibrinogen required for generating the desired numbers of constructs. Each construct is generated from 200 μ l fibrinogen and 500 μ l thrombin solution.
- c. Commence by creating the thrombin solution by adding thrombin (200U) to a 50 ml tube containing the cell culture medium at a ratio of 50 μ l/ml solution.
- d. Add the anti-fibrinolytic agents aminohexanoic acid (200 mM) and aprotinin (10 mg/ml) to the thrombin solution at a ratio of 2 μ l/ml in order to reduce the degradation rate of the fibrin gel, in order for it to match the rate of new matrix formation so that the mechanical integrity of the tissue can be maintained over longer periods of time.
- e. Pipette 500 μ l of the thrombin solution to each well and tilt the plates/dishes to ensure the bottom surfaces of the wells are fully covered and that there are no gaps or bubbles.
- f. Quickly pipette 200 μ l fibrinogen into each well and gently mix by rotating the plates for 1 second to allow the two components to mix.
- g. Quickly place the plates inside the 37°C, 5% CO₂ humidity incubator and allow gels to polymerize for approximately 30 minutes. Thrombin cleaves small peptides from the fibrinogen chain, producing soluble fibrin monomers, which then cross-link into an insoluble, polymerized fibrin clot.
- h. Proceed with cell isolation during this time.

6. Isolation of cells from culture flasks

- a. Carefully remove the growth medium from the flasks using a 10 ml serological pipette.
- b. Wash the cells gently by adding 5 ml of sterile PBS for 2-3 seconds to remove cell debris and remaining medium and tilt the flask gently.
- c. Aspirate and discard the PBS.
- d. Isolate cells from T175 culture flasks by applying 7 ml of TrypLE Select enzyme solution (or 1 ml per 25 cm² of growth area e.g. 1 ml for a T25 culture flask; 3 ml for T75).

Critical Parameter

This enzyme has an increased purity and hence specificity for cellular bonds compared to other traditional dissociation agents such as Trypsin, making it less likely to produce cellular damage. It also considerably enhances the replication capacity of primary cells.

- e. Place the flasks in a 37°C incubator for 3 minutes to allow activation of the enzyme and cell detachment.
- f. Add an equal amount (e.g. 7 ml) of growth medium containing 10% FBS to the flasks in order to inactivate the enzyme.
- g. Add the liquid containing the detached cells to a 50 ml sterile tube.
- h. Balance and centrifuge the cell solution at 1000 RPM for 3 minutes to pellet the cells.
- i. Carefully aspirate the supernatant inside the flow hood using a 10 ml serological pipette.
- j. Gently re-suspend cells in 10 ml of fresh D10 growth medium.

- k. Cells are ready to be seeded into constructs.

7. Determination of cell numbers

- a. Determine the number of cells per ml using the Trypan-Blue dye exclusion test.
- b. Mix 10 µl of the cell suspension with an equal part of 0.4% Trypan Blue inside a clean standard 48-well plate.
- c. Add 10 µl of the mix into one of the two compartments of a counting slide suitable for the automated cell counter, in this case a Countess automated cell counter.
- d. Insert the slide into the cell counter to obtain the total cell count, viable cell count and the concentration of cells/ml.
- e. Record the number of viable cells/ml.
- f. Repeat the measurement using the second slide chamber.
- g. Average the number of viable cells/ml between the two readings.
Critical parameter
Make sure that the viability is not lower than 85%, an average between 90-97% is to be expected.
- h. Dilute the cell solution appropriately using 10% DMEM in order to reach a concentration of 100.000 cells/ml.

8. Generation of final constructs

See Figure 3 for a schematic representation of the steps described here.

- a. Seed the cells on top of the fibrin constructs immediately following gel polymerization, at a density of 100K/ml of cell culture medium.
- b. Use non-cell seeded constructs as controls.
- c. Top up each well with an additional 1 ml of culture medium to ensure constructs are covered.
- d. Top up each well in the control plates with 2 ml of culture medium.
- e. Close the lids and place inside the 37°C, 5% CO₂ humidity incubator.
- f. Allow the cells to attach to the scaffolds for at least 2 days.
- g. Replace the medium with 2 ml of fresh (supplemented) DMEM not earlier than 2 days after the constructs were developed.
- h. Continue to replace the medium every 2-3 days for the duration of culture.

9. Osteogenic supplementation of constructs

- a. Determine a time for commencement of supplementation suitable for the research question (i.e. 7 days, 1 month).
- b. Supplement constructs with DMEM low glucose containing β-glycerophosphate (10 mM), ascorbic acid (0.1 mM) and dexamethasone (10 nM).
- c. Continue to replace the medium with 2 ml of osteogenic DMEM every 2-3 days.

ALTERNATE PROTOCOL 1

MODIFICATION OF THE SYSTEM WITH ALTERNATIVE CELL POPULATIONS

These short guidelines describe the application of alternative cellular populations to the system to produce similar bone constructs, heterogeneous cell constructs or different types of tissues.

Materials

Same as Basic Protocol 1, with the addition of the desired primary/cell line population(s) of interest and their corresponding culture medium and supplementation regime.

Protocol steps

Embedding of immortalised cell lines

1. Osteoblastic cell lines such as MC3T3-E1/2T3 from the European Collection of Authenticated Cell Cultures (ECACC) can be used for producing bone constructs more rapidly.
2. Undertake a series of optimisation tests to determine a suitable number of cells to be applied to gels, as osteoblastic cell lines can digest the fibrin matrix quickly, making it difficult to culture constructs for periods longer than 1 month.
3. Culture cells according to standard procedures in Minimal Essential Medium Eagle (MEM) Alpha Modification (10% FBS, 1% P/S, 2.4% L-glutamine).

Embedding of stem cells

1. Apply mesenchymal stromal cells (murine or human-derived) to constructs using the standard procedures.
2. Use a growth medium and supplementation regime suitable for differentiating the embedded cells into the chosen phenotype.

Embedding of co-cultures

1. Undertake a series of viability assays in 2D, while culturing individual and mixed populations of cells in each of their corresponding types of culture medium and in mixed, equal parts of each medium.

2. Record results and analyse viability to determine medium compatibility with cells and thus adjust the culture protocol as necessary.
3. Apply the cells to constructs using the standard procedures.

REAGENTS AND SOLUTIONS

Preparation of the digestion cocktail for isolating osteoprogenitor cells

1. Prepare an enzymatic digestion cocktail for extracting osteoprogenitor cells from the periosteum of femurs by dissolving 2.5 mg/ml collagenase I, 0.7 mg/ml collagenase II and 0.5 units/ml dispase I, in sterile PBS. The volume of the liquid needs to be sufficient for the bones to be fully immersed. That is approximately 12 ml in a standard 15 ml tube.

Critical Parameter

The digestion cocktail needs to be prepared before the time the rats are culled and received to prevent delays and ensure maximal cell viability.

2. Aspirate the solution using a 10 ml syringe and pass the solution through a standard 0.22 µm filter.

Preparation of the culture media

1. Prepare one 500 ml bottle of DMEM High Glucose containing 20% serum (D20) and 1% penicillin-streptomycin by removing 105 ml of medium and replacing it with 100 ml of FBS and 5 ml of the antibiotic solution.
2. Prepare one 500 ml bottle of DMEM High Glucose containing 10% serum (D10) and 1% penicillin-streptomycin by removing 55 ml of medium and replacing it with 50 ml of FBS and 5 ml of the antibiotic solution.

Preparation of osteogenic medium

1. Prepare one 500 ml bottle of DMEM Low Glucose containing 10% serum (D20), 1% penicillin-streptomycin, β-glycerophosphate (10 mM), ascorbic acid (0.1 mM) and dexamethasone (10 nM) (Sigma Aldrich, Germany), to encourage new matrix deposition along the entire length of the constructs.

Preparation of the thrombin component

1. Reconstitute the bovine-derived thrombin powder (1KU) using 0.1% w/v BSA in 5 ml F12K Nutrient Mixture (1X) with Kaighn’s Modification to make a final concentration of 200 U/ml.
2. Aspirate the solution using a 1 ml syringe and pass it through a 0.22 µm filter several times, collecting the filtered solution in a sterile 5 ml tube.

Critical Parameter

This step has to be performed slowly and using a smaller volume syringe to prevent blocking the filter with thrombin. If this happens, thrombin needs to be prepared anew.

3. Prepare 1 ml aliquots to prevent repeated thawing.
4. Store immediately at -20°C until use.

Preparation of the fibrinogen component

1. Commence by preparing a stock of approximately 50 ml fibrinogen solution.
2. Reconstitute the powdered bovine fibrinogen in F12K Nutrient Mixture (1X) with Kaighn's Modification at a ratio of 20 mg/ml inside a 50 ml sterile tube.
3. Place in a 37°C waterbath for 1-2 hours, gently swirling every 30 minutes to allow for the slow dissolution of the fibrinogen powder.
4. Divide the stock into aliquots of 10 ml inside sterile 50 ml tubes.
5. Sterilise the solutions by connecting each of the 50 ml tubes to a Millipore Steriflip 50 ml filtration unit containing a 0.22 µm filter.
6. Store immediately at -20°C until use. Repeated thawing is not recommended.

Preparation of aminohexanoic acid

1. Dissolve powder in PBS to a concentration of 200 mM.
2. Sterilise by passing through a 0.22 µm filter.
3. Aliquot in smaller amounts as repeated thawing is not recommended.
4. Store at -20°C until use.

Preparation of aprotinin

1. Dissolve in PBS to a concentration of 10 mg/ml.
2. Sterilise by passing through a 0.22 µm filter.
3. Aliquot in smaller amounts as repeated thawing is not recommended.
4. Store at -20°C until use.

Preparation of ascorbic acid

1. Prepare stock solution from powder in PBS.
2. Sterilise by passing through a 0.22 µm filter.
3. Aliquot in smaller amounts as repeated thawing is not recommended.
4. Store at -20°C until use.

Preparation of β -glycerophosphate

1. Prepare stock solution from powder in PBS.
2. Sterilise by passing through a 0.22 μ m filter.
3. Aliquot in smaller amounts as repeated thawing is not recommended.
4. Store at -20°C until use.

Preparation of Dexamethasone

1. Prepare a stock solution of dexamethasone by diluting the powder in absolute EtOH at a ratio of 1 ml EtOH per mg of dexamethasone.
2. If necessary, sterilise by passing through a 0.22 μ m filter.
3. Aliquot in smaller amounts as repeated thawing is not recommended.
4. Store at -20°C until use.

Preparation of orthophosphoric acid (3.5 M)

1. Prepare 3.5 M orthophosphoric acid in molecular grade or deionised H₂O.
2. Cool before use for 1 hour at 2-8°C.

COMMENTARY

Background Information

The fibrin contraction approach to forming 3D tissues that underpins this organotypic bone system has been created and diversified over the past 8 years to suit a variety of cell phenotypes (Huang, Dennis et al. 2005, Paxton, Donnelly et al. 2010, Paxton, Grover et al. 2010, Mehrban, Paxton et al. 2011, Paxton, Wudebwe et al. 2012, Bannerman, Paxton et al. 2014, Koburger, Bannerman et al. 2014, Lebled, Grover et al. 2014, Wudebwe, Bannerman et al. 2015, Wang, Williams et al. 2016, Baar 2017, Shaw, Lee-Barthel et al. 2017, Iordachescu, Amin et al. 2018, Iordachescu, Hulley et al. 2018). The system was initially developed to grow replacement ligaments and tendons for eventual implantation into humans (Paxton, Donnelly et al. 2010, Paxton, Grover et al. 2010, Paxton, Wudebwe et al. 2012, Lebled, Grover et al. 2014, Wang, Williams et al. 2016). It then diversified into models to facilitate basic science research into hard-soft tissue interfaces, sports physiology and sports rehabilitation (Baar 2017, Shaw, Lee-Barthel et al. 2017). The model has also been used to form muscle tissue (Huang, Dennis et al. 2005), but its impact has been in the translation of findings. Baar and colleagues have been using the tendon model to design new nutritional and training regimes for professional athletes in order to maximise performance, decrease the risk of tendon/ligament injury and accelerate the return to play (Baar 2017, Shaw, Lee-Barthel et al. 2017).

This protocol summarised the adaptation of this technology to form bone-like tissue containing mature matrix and cells and to maintain their viability over significant periods of time. Although primary

osteoblast to osteocyte cell transition has recently been reported in 3D using various technologies (Boukhechba, Balaguer et al. 2009, Gu, Zhang et al. 2015, Sun, Gu et al. 2015, Mc Garrigle, Mullen et al. 2016), our model differs in the close recapitulation of complex *in-vivo* conditions and in the self-structuring process as opposed to a pre-formed organic-inorganic matrix template. The ability to recreate such features resembling *in vivo* biochemistry and micro-anatomy could significantly diminish the need for use of animal models in skeletal research. It might also provide a tool to investigate/re-evaluate promising compounds.

Additional features of the system are summarised below.

Advantages

1. The system allows the growth of bone-like tissue at the cm scale.
2. Constructs can be grown for extensive periods of time exceeding 1 year.
3. It is possible to differentiate embedded cells to a terminal phenotype and maintain it over the culture period.
4. Allows cells to organise along the mechanical axis, as seen in bone.
5. Allows the study of early matrix production.
6. Responsive to drugs and many other molecules.
7. Can be used with cells from a wide range of species.
8. Adaptable to a whole range of cell phenotypes.
9. Allows the growth of endothelial tubes.
10. Can be mechanically tested.
11. Contains mineral phases which transition to hydroxyapatite, the mature bone mineral.
12. Requires minimal amounts of new materials.
13. Does not require modifications of the kit already present in cell culture facilities.
14. Does not require a large number or primary cells.
15. Can reduce the number of animals used for this type of research.

Limitations

1. Requires further optimisation to enhance mechanical resistance.
2. Relatively flat, sheet-like structure but provides significant advantages for 3D imaging and mapping.

Critical Parameters

The production of the mineral component (Step 1) as well as coating of the plates with silicone elastomer (Step 2) need to be performed at least 2 weeks before fibrin construct generation, to allow these components to fully cure and set. The assembly of the two components (Step 3) should also be performed well in advance as they require 70% ethanol (and) UV sterilization

1
2
3
4
5
6
7
8
9
10
11
12
13
14
15
16
17
18
19
20
21
22
23
24
25
26
27
28
29
30
31
32
33
34
35
36
37
38
39
40
41
42
43
44
45
46
47
48
49
50
51
52
53
54
55
56
57
58
59
60

overnight. Improper sterilisation of the plates can lead to contamination and ethanol residue that has not been allowed to fully dry might affect the cells.

The use of an automated cell counter is recommended during construct set-up (Step 4), to allow mass production of these constructs and rapid quantification of isolated cells during the short time frame during which fibrin gels are polymerised; which also helps maximise the viability of isolated cells. Care must be taken during aspiration of supernatant from cell pellets (Step 4) following isolation as an insufficient number of cells may compromise the experiment and fibrin gels need to be used immediately after production (i.e. cannot be frozen or re-scheduled for use). Ensure the viability percentage of the cell population (Step 7) is not less than 85% before embedding into fibrin gels.

When sterilising the thrombin solution using a 0.22 m filter, ensure you drive the 1 ml syringe slowly, to prevent the filter getting blocked. If this occurs, a new thrombin batch needs to be prepared.

The digestion cocktail for isolating periosteal cells needs to be prepared in advance, before the rats are culled, to ensure maximal viability.

Troubleshooting

Problems that may arise at different steps and their solutions are listed below.

Step	Problem	Solution
1 i	Pins cannot be inserted due to cement hardening	Cool the anchor moulds on top of ice blocks for at least 30 minutes to slow the hardening reaction
4 q	Cells do not reach 70% confluency within 2-3 days	Ensure the medium is replaced every 2 days after 3 days of culture
5 g	Gels have not polymerised uniformly	Thrombin and Fibrinogen have not been mixed properly – repeat this step
8	Gels are not contracting following cell seeding	Repeat the work ensuring that: <ol style="list-style-type: none">1. Gels are not left to polymerise for longer than necessary, as they might attach to the elastomer base2. You have applied the correct number of viable cells

Understanding Results

Self-organisation

Constructs undergo a process of contraction from the edges following addition of the cells, which completes around day 7 of culture (Figure 3 right). Constructs which are not seeded with cells can be used as controls and display a small degree of contraction that is not significant or structured (Figure 3 right). Additionally, control constructs which are developed with cells but do not contain anchors contract maximally into spherical structures, as opposed to longitudinal, cylindrical structures (Figure 4). Contraction against the anchors is particularly important for simulating the architecture of bone tissue (Figure 5), which contains mineralised matrix and cells arranged in a hierarchical fashion. The two retention points in the form of two ceramic anchors allow the cells to remodel the fibrin scaffold (Figure 6a), creating tensile forces that lead to cellular and molecular alignment along the line of tension (b-d). Moreover, a spiralling pattern of contraction from the edges (shown in Figure 6 b-c) leads to the formation of basic osteonal-like structures (e), which is particularly useful as it allows the cells to become embedded in a structure more similar to the native tissue and also to simulate the level of entrapment of terminally differentiated, osteocytic-like cells which can be grown using this model (f).

Early events

The deposition of collagen in constructs is important as it is an indicator of the initiation of ossification. Collagen will be detected mainly adjacent to the anchors during the first month of culture, and will be observed progressing towards the center with extended culture times and further osteogenic supplementation until the two parts meet centrally, thus recapitulating steps from the fracture repair cascade (a summary is provided in Figure 11). Several whole-mount stains can be applied to detect the presence of collagen in constructs. Collagen can also be visualised non-destructively by using second harmonic imaging (Figure 7a), an optical effect generated by the unique molecular structure of collagen when exposed to a laser of infrared-near infrared wavelength. This effect can be recorded at half the wavelength of the incoming laser (7b) and the technique can be combined with two-photon excitation fluorescence to simultaneously visualise cells, stained with Calcein AM. Collagen appears as pockets (7b) surrounded by cellular structures.

Evolution of mineralisation

Mineralisation can also be detected in constructs using several whole-mount stains including Alizarin Red. Non-destructively, it can be visualised using technologies such as X-Ray Fluorescence or micro-X-Ray fluorescence, which allow the mapping of individual chemical elements associated with the mineral and osteoid. Each element presents a different emission line upon being exposed to X-Ray radiation

(Figure 8a), which is recorded and quantified. Figure 8b provides examples of the expected results, with calcium and phosphorus progressing from the anchors towards the center over the first month of culture and co-localised with sulphur, indicative of the protein-rich matrix. This can also be visualised using histological methods.

Chemical identification of the matrix composition

The characteristics of the newly forming matrix can be probed using a range of techniques, including immunohistochemistry, mass spectrometry and PCR. For non-invasive visualisation of different chemical groups forming in constructs as well as their stage of development and association with other components (i.e the mineral phase), Raman Spectroscopy is an ideal method. The technique works by recording the photons which have been inelastically scattered upon excitation with a monochromatic laser (Figure 9a). Different chemical groups can be identified based on signature peaks, which can also be mapped across the entire length of constructs, giving valuable information on the spatial localisation of biological material. Figure 9b presents examples of maps of an area from the interface region of a 7-days old construct, which contain a fragment of the anchor and the soft tissue surrounding it. The maps are generated based on spectral peaks of chemical groups associated with the organic matrix, such as phenylalanine (peak chosen located within the band $990 - 1007 \text{ cm}^{-1}$) and amide I associated with collagen (peak chosen located within the band $1580 - 1617 \text{ cm}^{-1}$) as well as chemical groups associated with the mineral component, such as tri-calcium phosphate (chosen band $1015 - 1045 \text{ cm}^{-1}$). The spatial distribution of different groups can be compared and linked to results from other mapping or optical techniques, including immunohistochemical information from other biological components.

Long-term characterisation of bone formation

Constructs can be grown for durations that can be clinically-useful (over 1 year), during which time extensive development of the matrix and cells takes place. However, the matrix is fully mineralised as early as 3 months (Figure 10a), with noticeable changes in matrix composition and stiffness continuing to take place over the subsequent months (b). At the end of a year in culture, a very dense outer matrix can be observed. Previous work has identified that the mineral accounts for approximately 70% of the weight of constructs at this stage (Iordachescu, Amin et al. 2018).

A major advantage of this technique is the ability to monitor and chemically characterise ossification longitudinally (d, left, middle). Secondly, the co-culture of different cell types is possible, including human umbilical vein endothelial cells (d right), which form tubular structures lengthwise, and which could be further optimised to develop a vascularised bone tissue model.

In terms of mature bone cells, osteocytic features are detectable as early as 3 months of culture, with long connecting projections (e) that are able to attach to the matrix and survive during the year in culture (f). These projections run deep inside the matrix, a structural feature that can be observed using both traditional histological techniques but also higher resolution optical technologies such as Synchrotron Radiation Computed Tomography (g). Figure 10 g presents examples of these channels linking to lacunar – like structures where osteocytes reside.

1
2
3
4
5
6
7
8
9
10
11
12
13
14
15
16
17
18
19
20
21
22
23
24
25
26
27
28
29
30
31
32
33
34
35
36
37
38
39
40
41
42
43
44
45
46
47
48
49
50
51
52
53
54
55
56
57
58
59
60

Time Considerations

- Step 1** 2-3 hours for generating approx. 100 anchors
 Allow extra 3-4 hours for cement to fully harden
- Step 2** 2-3 hours for coating approx. 20 x 6-well plates
 Allow a minimum of 1 week for base to polymerise at room temperature
- Step 3** Approx. 2-3 hours for assembling 10 x 6-well plates (60 constructs)
- Step 4** 3-4 hours including 1 hour incubation time
 Allow 3-4 days for cells to reach confluency
- Step 5** 30 minutes for every 10 x 6- well plates (60 constructs)
- Step 6** 20 minutes
- Step 7** 10 minutes
- Step 8** 20 minutes for every 10 x 6- well plates (60 constructs)
- Step 9** 20 minutes for every 10 x 6- well plates (60 constructs)

ACKNOWLEDGEMENT

This research was funded by a National Centre for the Replacement Refinement and Reduction of animals in research (NC3Rs) grant (NC/L001403/1). Authors would like to thank Professor Owen Addison (School of Dentistry, University of Birmingham) and Dr Alexandra Pacureanu (X-ray Nanoprobe Group, European Synchrotron Radiation Facility) for support with Synchrotron Computed Tomography image acquisition.

LITERATURE CITED

- Ahmed, T., R. Ringuelette, V. Wallace and M. Griffith (2015). "Autologous fibrin glue as an encapsulating scaffold for delivery of retinal progenitor cells." *Frontiers in Bioengineering and Biotechnology* **2**(85).
- Anthonissen, J., C. Ossendorf, J. L. Hock, C. T. Steffen, H. Goetz, A. Hofmann and P. M. Rommens (2016). "The role of muscular trauma in the development of heterotopic ossification after hip surgery: An animal-model study in rats." *Injury* **47**(3): 613-616.
- Baar, K. (2017). "Minimizing Injury and Maximizing Return to Play: Lessons from Engineered Ligaments." *Sports Medicine (Auckland, N.z.)* **47**(Suppl 1): 5-11.
- Bannerman, A., J. Z. Paxton and L. M. Grover (2014). "Imaging the hard/soft tissue interface." *Biotechnol Lett* **36**(3): 403-415.
- Bellows, C. G., J. E. Aubin, J. N. Heersche and M. E. Antosz (1986). "Mineralized bone nodules formed in vitro from enzymatically released rat calvaria cell populations." *Calcif Tissue Int* **38**(3): 143-154.
- Bouet, G., M. Cruel, C. Laurent, L. Vico, L. Malaval and D. Marchat (2015). "Validation of an in vitro 3D bone culture model with perfused and mechanically stressed ceramic scaffold." *Eur Cell Mater* **29**: 250-266; discussion 266-257.
- Boukhechba, F., T. Balaguer, J.-F. Michiels, K. Ackermann, D. Quincey, J.-M. Boulter, W. Pyerin, G. F. Carle and N. Rochet (2009). "Human Primary Osteocyte Differentiation in a 3D Culture System." *Journal of Bone and Mineral Research* **24**(11): 1927-1935.
- Buttery, L. D., S. Bourne, J. D. Xynos, H. Wood, F. J. Hughes, S. P. Hughes, V. Episkopou and J. M. Polak (2001). "Differentiation of osteoblasts and in vitro bone formation from murine embryonic stem cells." *Tissue Eng* **7**(1): 89-99.
- Chesnutt, B. M., A. M. Viano, Y. Yuan, Y. Yang, T. Guda, M. R. Appleford, J. L. Ong, W. O. Haggard and J. D. Bumgardner (2009). "Design and characterization of a novel chitosan/nanocrystalline calcium phosphate composite scaffold for bone regeneration." *J Biomed Mater Res A* **88**(2): 491-502.
- Drury, J. L. and D. J. Mooney (2003). "Hydrogels for tissue engineering: scaffold design variables and applications." *Biomaterials* **24**(24): 4337-4351.
- Edmondson, R., J. J. Broglie, A. F. Adcock and L. Yang (2014). "Three-Dimensional Cell Culture Systems and Their Applications in Drug Discovery and Cell-Based Biosensors." *Assay and Drug Development Technologies* **12**(4): 207-218.
- Einhorn, T. A. and L. C. Gerstenfeld (2015). "Fracture healing: mechanisms and interventions." *Nat Rev Rheumatol* **11**(1): 45-54.
- Eyrich, D., F. Brandl, B. Appel, H. Wiese, G. Maier, M. Wenzel, R. Staudenmaier, A. Goepferich and T. Blunk (2007). "Long-term stable fibrin gels for cartilage engineering." *Biomaterials* **28**(1): 55-65.
- Eyrich, D., A. Göpferich and T. Blunk (2007). Fibrin in Tissue Engineering. *Tissue Engineering*. J. P. Fisher. Boston, MA, Springer US: 379-392.
- Ghosh-Choudhury, N., J. J. Windle, B. A. Koop, M. A. Harris, D. L. Guerrero, J. M. Wozney, G. R. Mundy and S. E. Harris (1996). "Immortalized murine osteoblasts derived from BMP 2-T-antigen expressing transgenic mice." *Endocrinology* **137**(1): 331-339.
- Gu, Y., W. Zhang, Q. Sun, Y. Hao, J. Zilberberg and W. Y. Lee (2015). "Microbeads-Guided Reconstruction of 3D Osteocyte Network during Microfluidic Perfusion Culture." *J Mater Chem B* **3**(17): 3625-3633.

- Huang, Y. C., R. G. Dennis, L. Larkin and K. Baar (2005). "Rapid formation of functional muscle in vitro using fibrin gels." J Appl Physiol (1985) **98**(2): 706-713.
- Iordachescu, A., H. D. Amin, S. M. Rankin, R. L. Williams, C. Yapp, A. Bannerman, A. Pacureanu, O. Addison, P. A. Hulley and L. M. Grover (2018). "An In Vitro Model for the Development of Mature Bone Containing an Osteocyte Network." Advanced Biosystems **2**(2): n/a-n/a.
- Iordachescu, A., P. Hulley and L. Grover (2018). "A novel method for the collection of nanoscopic vesicles from an organotypic culture model." RSC Advances **8**(14): 7622-7632.
- Janmey, P. A., J. P. Winer and J. W. Weisel (2009). "Fibrin gels and their clinical and bioengineering applications." J R Soc Interface **6**(30): 1-10.
- Kan, L. and J. A. Kessler (2011). "Animal Models of Typical Heterotopic Ossification." Journal of Biomedicine and Biotechnology **2011**: 309287.
- Kaplan, F. S., E. M. Shore, R. J. Pignolo and D. L. Glaser (2005). "Animal models of fibrodysplasia ossificans progressiva." Clinical Reviews in Bone and Mineral Metabolism **3**(3): 229-234.
- Kato, Y., J. J. Windle, B. A. Koop, G. R. Mundy and L. F. Bonewald (1997). "Establishment of an Osteocyte-like Cell Line, MLO-Y4." Journal of Bone and Mineral Research **12**(12): 2014-2023.
- Kikuchi, M., S. Itoh, S. Ichinose, K. Shinomiya and J. Tanaka (2001). "Self-organization mechanism in a bone-like hydroxyapatite/collagen nanocomposite synthesized in vitro and its biological reaction in vivo." Biomaterials **22**(13): 1705-1711.
- Koburger, S., A. Bannerman, L. M. Grover, F. A. Müller, J. Bowen and J. Z. Paxton (2014). "A novel method for monitoring mineralisation in hydrogels at the engineered hard-soft tissue interface." Biomaterials Science **2**(1): 41-51.
- Kodack, D. P., A. F. Farago, A. Dastur, M. A. Held, L. Dardaei, L. Friboulet, F. von Flotow, L. J. Damon, D. Lee, M. Parks, R. Dicecca, M. Greenberg, K. E. Kattermann, A. K. Riley, F. J. Fintelman, C. Rizzo, Z. Piotrowska, A. T. Shaw, J. F. Gainor, L. V. Sequist, M. J. Niederst, J. A. Engelman and C. H. Benes (2017). "Primary Patient-Derived Cancer Cells and Their Potential for Personalized Cancer Patient Care." Cell Reports **21**(11): 3298-3309.
- Lebled, C., L. M. Grover and J. Z. Paxton (2014). "Combined decellularisation and dehydration improves the mechanical properties of tissue-engineered sinews." J Tissue Eng **5**: 2041731414536720.
- Lee, K. Y. and D. J. Mooney (2001). "Hydrogels for Tissue Engineering." Chemical Reviews **101**(7): 1869-1880.
- Lee, L.-T., P.-C. Kwan, Y.-F. Chen and Y.-K. Wong (2008). "Comparison of the Effectiveness of Autologous Fibrin Glue and Macroporous Biphasic Calcium Phosphate as Carriers in the Osteogenesis Process With or Without Mesenchymal Stem Cells." Journal of the Chinese Medical Association **71**(2): 66-73.
- Liu, M., X. Zeng, C. Ma, H. Yi, Z. Ali, X. Mou, S. Li, Y. Deng and N. He (2017). "Injectable hydrogels for cartilage and bone tissue engineering." **5**: 17014.
- Maas, M., P. Guo, M. Keeney, F. Yang, T. M. Hsu, G. G. Fuller, C. R. Martin and R. N. Zare (2011). "Preparation of mineralized nanofibers: collagen fibrils containing calcium phosphate." Nano Lett **11**(3): 1383-1388.
- Matthews, B. G., D. Naot, K. E. Callon, D. S. Musson, R. Locklin, P. A. Hulley, A. Grey and J. Cornish (2014). "Enhanced osteoblastogenesis in three-dimensional collagen gels." BoneKEY Rep **3**.
- Mc Garrigle, M. J., C. A. Mullen, M. G. Haugh, M. C. Voisin and L. M. McNamara (2016). "Osteocyte differentiation and the formation of an interconnected cellular network in vitro." Eur Cell Mater **31**: 323-340.
- Mehrban, N., J. Z. Paxton, J. Bowen, A. Bolarinwa, E. Vorndran, U. Gbureck and L. M. Grover (2011). "Comparing physicochemical properties of printed and hand cast biocements designed for ligament replacement." Advances in Applied Ceramics **110**(3): 162-167.
- Mitra, A., L. Mishra and S. Li (2013). "Technologies for deriving primary tumor cells for use in personalized cancer therapy." Trends in biotechnology **31**(6): 347-354.

- Mizutani, A., I. Sugiyama, E. Kuno, S. Matsunaga and N. Tsukagoshi (2001). "Expression of matrix metalloproteinases during ascorbate-induced differentiation of osteoblastic MC3T3-E1 cells." J Bone Miner Res **16**(11): 2043-2049.
- Moreau, J. L., M. D. Weir and H. H. K. Xu (2009). "Self-setting collagen-calcium phosphate bone cement: Mechanical and cellular properties." Journal of Biomedical Materials Research Part A **91A**(2): 605-613.
- Neves, L. S., M. T. Rodrigues, R. L. Reis and M. E. Gomes (2016). "Current approaches and future perspectives on strategies for the development of personalized tissue engineering therapies." Expert Review of Precision Medicine and Drug Development **1**(1): 93-108.
- Paxton, J. Z., K. Donnelly, R. P. Keatch, K. Baar and L. M. Grover (2010). "Factors Affecting the Longevity and Strength in an In Vitro Model of the Bone–Ligament Interface." Annals of Biomedical Engineering **38**(6): 2155-2166.
- Paxton, J. Z., L. M. Grover and K. Baar (2010). "Engineering an in vitro model of a functional ligament from bone to bone." Tissue Eng Part A **16**(11): 3515-3525.
- Paxton, J. Z., U. N. Wudebwe, A. Wang, D. Woods and L. M. Grover (2012). "Monitoring sinew contraction during formation of tissue-engineered fibrin-based ligament constructs." Tissue Eng Part A **18**(15-16): 1596-1607.
- Perka, C., S. Stern, R.-S. Spitzer and K. Lindenhayn (2003). Chondrocytes and Fibrin Glue. Cartilage Surgery and Future Perspectives. C. Hendrich, U. Nöth and J. Eulert. Berlin, Heidelberg, Springer Berlin Heidelberg: 151-155.
- Rahaman, M. N., D. E. Day, B. S. Bal, Q. Fu, S. B. Jung, L. F. Bonewald and A. P. Tomsia (2011). "Bioactive glass in tissue engineering." Acta Biomater **7**(6): 2355-2373.
- Reznikov, N., H. Chase, V. Brumfeld, R. Shahar and S. Weiner (2015). "The 3D structure of the collagen fibril network in human trabecular bone: relation to trabecular organization." Bone **71**: 189-195.
- Shaw, G., A. Lee-Barthel, M. L. R. Ross, B. Wang and K. Baar (2017). "Vitamin C-enriched gelatin supplementation before intermittent activity augments collagen synthesis." The American Journal of Clinical Nutrition **105**(1): 136-143.
- Sowa, H., H. Kaji, T. Yamaguchi, T. Sugimoto and K. Chihara (2002). "Smad3 promotes alkaline phosphatase activity and mineralization of osteoblastic MC3T3-E1 cells." J Bone Miner Res **17**(7): 1190-1199.
- Sun, Q., Y. Gu, W. Zhang, L. Dziopa, J. Zilberberg and W. Lee (2015). "Ex vivo 3D osteocyte network construction with primary murine bone cells." Bone Research **3**: 15026.
- Šupová, M. (2009). "Problem of hydroxyapatite dispersion in polymer matrices: a review." Journal of Materials Science: Materials in Medicine **20**(6): 1201-1213.
- Thein-Han, W., J. Liu and H. H. Xu (2012). "Calcium phosphate cement with biofunctional agents and stem cell seeding for dental and craniofacial bone repair." Dent Mater **28**(10): 1059-1070.
- Ueno, T., T. Kagawa, M. Kanou, T. Fujii, J. Fukunaga, N. Mizukawa, T. Sugahara and T. Yamamoto (2003). "Immunohistochemical observations of cellular differentiation and proliferation in endochondral bone formation from grafted periosteum:: expression and localization of BMP-2 and -4 in the grafted periosteum." Journal of Cranio-Maxillofacial Surgery **31**(6): 356-361.
- Vazquez, M., B. A. J. Evans, D. Riccardi, S. L. Evans, J. R. Ralphs, C. M. Dillingham and D. J. Mason (2014). "A New Method to Investigate How Mechanical Loading of Osteocytes Controls Osteoblasts." Frontiers in Endocrinology **5**: 208.
- Wahl, D. A. and J. T. Czernuszka (2006). "Collagen-hydroxyapatite composites for hard tissue repair." Eur Cell Mater **11**: 43-56.
- Wang, A., R. L. Williams, N. Jumbu, J. Z. Paxton, E. T. Davis, M. A. Snow, A. Campbell Ritchie, C. B. Johansson, R. L. Sammons and L. M. Grover (2016). "Development of tissue engineered ligaments with titanium spring reinforcement." RSC Advances **6**(100): 98536-98544.

Wang, H., M. Bongio, K. Farbod, A. W. Nijhuis, J. van den Beucken, O. C. Boerman, J. C. van Hest, Y. Li, J. A. Jansen and S. C. Leeuwenburgh (2014). "Development of injectable organic/inorganic colloidal composite gels made of self-assembling gelatin nanospheres and calcium phosphate nanocrystals." Acta Biomater **10**(1): 508-519.

Wang, P., L. Zhao, J. Liu, M. D. Weir, X. Zhou and H. H. K. Xu (2014). "Bone tissue engineering via nanostructured calcium phosphate biomaterials and stem cells." **2**: 14017.

Wang, Y.-H., Y. Liu, P. Maye and D. W. Rowe (2006). "Examination of Mineralized Nodule Formation in Living Osteoblastic Cultures Using Fluorescent Dyes." Biotechnology progress **22**(6): 1697-1701.

Weinbaum, S., S. C. Cowin and Y. Zeng (1994). "A model for the excitation of osteocytes by mechanical loading-induced bone fluid shear stresses." J Biomech **27**(3): 339-360.

Wudebwe, U. N. G., A. Bannerman, P. Goldberg-Opppenheimer, J. Z. Paxton, R. L. Williams and L. M. Grover (2015). "Exploiting cell-mediated contraction and adhesion to structure tissues in vitro." Philosophical Transactions of the Royal Society B: Biological Sciences **370**.

Ye, Q., G. Zund, P. Benedikt, S. Jockenhoevel, S. P. Hoerstrup, S. Sakyama, J. A. Hubbell and M. Turina (2000). "Fibrin gel as a three dimensional matrix in cardiovascular tissue engineering." Eur J Cardiothorac Surg **17**(5): 587-591.

Zhao, S., Y. K. Zhang, S. Harris, S. S. Ahuja and L. F. Bonewald (2002). "MLO-Y4 osteocyte-like cells support osteoclast formation and activation." J Bone Miner Res **17**(11): 2068-2079.

FIGURE LEGENDS

Figure 1. Production of the template and moulds for anchor generation. Rectangular frames containing 4 horizontal rows of 5 trapezoidal shapes each can be printed in plastic using a regular 3D printer (a). These anchors can be up to 4 mm in height and approximately 4 mm x 2 mm in width (b). A standard impression silicone material can be formed on top of this template (c) to generate trapezoidal compartments where individual anchor moulds can be formed (d). The production of several moulds and templates allows the generation of a stock of ceramic anchors in preparation for the study (e).

Figure 2. Development of the mineral-fibrin backbone. 35 mm culture wells within 6-well culture dishes are used for developing each construct. Culture wells are coated with 1.5 ml of a silicone elastomer base and are allowed to dry at room temperature for 7 days on a flat surface to allow polymerization. Two anchors are attached to the silicone base using pins inserted during the formation process, at a distance of 1.5 cm from each other. Fibrin scaffolds are produced on the mineral backbone structure through the interaction of the normal plasma components thrombin and fibrinogen. Thrombin is added to a solution containing the cell culture medium and the anti-fibrinolytic agents aminohexanoic acid and aprotinin and 500 μ l are applied to each culture well. Hydrogels are generated by applying 200 μ l of fibrinogen on top of the thrombin solution. Gels are allowed to polymerize for 30 minutes during incubation at 37°C.

Figure 3. Development of constructs. Primary cells of an osteoprogenitor phenotype are seeded into the fibrin constructs immediately following gel polymerization, at a density of 100K/2ml of cell culture medium (left). The fibrin scaffold is reorganized around the retention points over the first week in culture (right, top panel). Control constructs, developed without cells show a small degree of contraction over 7 days, but remain as flat gels and do not assemble into 3D structures (right, bottom panel). Images are modified from Iordachescu, Amin et al. 2018 and are used under the terms of the Creative Commons Attribution Licence (CC-BY 4.0).

Figure 4. The presence of anchors is required for the formation of longitudinal structures. The two calcium phosphate anchors have a decisive role in matrix contraction and alignment. In the absence of anchors (illustrated in the diagram series in a, top row), cells maximally contract the fibrin scaffolds over three weeks into spherical structures (b, top image), whereas the provision of the 2 retention points (a, bottom row) allows the formation of a cylindrical structure in-between the two calcium phosphate structures (b, bottom image). Scale bars = 10 mm. Images in b are taken from (Wudebwe, Bannerman et al. 2015) and are used under the terms of the Creative Commons Attribution Licence (CC-BY 4.0).

Figure 5. Bone is a highly-organised tissue, from the nano to the macro scale. The image presents a simplified schematic of the organic-inorganic hierarchical structure in lamellar bone tissue. Collagen molecules (normally triple-helical, simplified here) are arranged end-to-end and parallel to each other (left image). These structures contain spaces of approximately 36 nm between them, which facilitate nucleation by apatitic crystals. Mineralised collagenous fibres make up concentric lamellae (middle), each containing collagen fibres orientated in a specific direction. These lamellae form osteons, which act as passageways for blood vessels (arteries and veins) and nerve fibres and are lined internally by the endosteum. Osteocytes, the mature bone cells, are arranged concentrically at the junctions between lamellae (right). They are embedded in lacunae and linked by canaliculi, which allow cell-to-cell communication and connect to the endosteum.

Figure 6. Multi-directional forces lead to self-structuring of constructs. Cells are able to adhere to and remodel the fibrin matrix, creating tensile forces between the two retention points and a spiral-like contraction pattern from the edges of the structures (b, c). Tension leads to cellular alignment along the loading forces (d), which is particularly useful for mimicking the hierarchical cellular organisation and matrix production in bone. Moreover, the longitudinal spiral-like reorganisation of the matrix (e) leads to the creation of basic osteonal-like structures (f), that is particularly useful at later points, when the inserted osteoprogenitor population becomes entrapped inside the highly mineralised matrix, maturing to an osteocytic phenotype (f) and creating canaliculi-like structures. Scale bars: d = 100 μ m. Image d is taken from Iordachescu, Amin et al. 2018 and is used under the terms of the Creative Commons Attribution Licence (CC-BY 4.0). Image e is modified from (Paxton, Wudebwe et al. 2012) and is used under the terms of the Creative Commons Attribution Licence (CC-BY).

Figure 7. Three dimensional visualisation of collagen deposits and cells in constructs. a, Mature collagen has a triple helical molecular structure which is non-centro-symmetrical. Thus, an incident monochromatic light emitted by a near-infrared laser which interacts with collagen creates an oscillating field at twice the frequency and half the wavelength, an optical effect known as second harmonic generation. b, This non-linear optical effect can therefore be visualised specifically at 432 nm (half the wavelength of the laser) corresponding to the purple-

blue area of the spectrum. Cellular structures fluorescently labelled with Calcein AM can be visualised simultaneously in the 481-577 nm region of the spectrum, corresponding to the light blue-green region. The image in b presents different angles of a 3D section acquired from the anchor region of 1 month-old constructs. This technique allows the non-destructive visualisation of the cell-matrix dynamics at the cellular resolution but over the tissue lengthscale, as the tissues are maturing and matrix undergoes ossification. Scale bars = 100 μ m.

Figure 8. Monitoring mineralisation over time. The initiation and development of mineralisation during the culture period can be monitored non-destructively using X-Ray fluorescence (in this case at the micron resolution), which can detect the presence of chemical elements such as Calcium (Ca) and Phosphorus (P), the main components of the mineral part of bone. a, X-Ray Fluorescence is generated following the ejection of a photoelectron from an atomic shell exposed to high-energy primary X-Ray radiation and the subsequent ‘jump’ of an outer electron from the near shells in order to fill this vacancy. The process is recorded as X-Ray Fluorescence, with different emission lines for each chemical element and different ‘jumps’ taking place between different shells (e.g. from the L to the K layer, known as the K α emission line; from M to K, known as K β etc). b, The pattern of localisation of Ca and P can be mapped using this technique and overlaid with that of chemical elements associated with proteins indicative of cellular matrix, such as Sulphur (S). The images in b present micro-XRF maps of live constructs over 21 days, based on Ca, P and S emission lines, which show the progression and co-localisation of Ca and P deposits (combined yellow) from the anchor towards the centre, while the sulphur-rich matrix is represented in blue. Scale bar = 4mm. Image b is taken from lordachescu, Amin et al. 2018 and is used under the terms of the Creative Commons Attribution Licence (CC-BY 4.0).

Figure 9. Creating compositional maps of tissues using Raman Spectroscopy. a, Raman spectroscopy relies on the process of inelastic scattering. This technique uses monochromatic light (laser) to excite photons to virtual energy states. When photons are scattered from a molecule most of them are elastically scattered (Rayleigh scattering), having the same energy (frequency and wavelength) as the incident photons. A very small proportion of these photons (1 in 10 million) are scattered inelastically (Raman scattering), which involves the loss (Stokes) or gain (anti-Stokes) of energy due to the interaction of light with vibrations associated with bonds within the sample. Chemical bonds have individual fingerprints that can be used for identification within biological samples and can be locally resolved and co-localised using high-resolution scans (b). Images in b present high-resolution maps of a section of a 7-day old construct, including a fragment of the anchor. These maps are based on the signals from chemical groups present in the organic matrix of constructs, such as phenylalanine (left), amide I present in the newly-forming collagen (middle); as well as the mineral component (tri-calcium phosphate, right) abundant in the anchor region. Scale bars = 1 mm.

Figure 10. Long term structural evaluation of constructs. Constructs can be grown for periods exceeding 1 year, making them useful for understanding normal and aberrant bone formation. a, As early as 3 months they display a mineral density similar to the calcium phosphate material of the anchor. b, The replacement of the initial matrix with mineralised collagen is visually noticeable, with 7 months-old mature constructs appearing strikingly different from the homogenous initial matrix. The matrix continues to ossify over the following months. Constructs which have been cultured for 1 year show a very dense and compact outer matrix (c). Some of the advantages of this culture system include the ability to monitor ossification longitudinally (d, left), the possibility to characterise these non-destructively in order to monitor the new organic matrix formation (middle, Raman map based on the CH₂ peak of collagen at 1447 cm⁻¹) and the adaptability of the model to include additional populations of cells, including human umbilical vein endothelial cells, which can give rise to tubular microstructures in the system. Another advantage of the system is the ability to differentiate cells to an osteocytic phenotype. Cells can be seen displaying a high number of interconnected projections at 3 months (e) which attach to the highly mineralised matrix (f, SEM image of cellular pods attaching to mineral spheres at 1 year) as well as projecting through it using canaliculi (g, top-bottom) and lacunar-like structures (g, middle) (synchrotron Computed Tomography image slices at a resolution of 100 nm). Scale bars: a = 2.5 mm; d = 100 μ m. Images c-d are modified from and e is taken from lordachescu, Amin et al. 2018 and are used under the terms of the Creative Commons Attribution Licence (CC-BY 4.0).

Figure 11. Simulating the fracture-repair process. This model recapitulates several steps of the fracture repair process, including 2 mechanical retention points, a blood clot-like microenvironment, as well as a source of periosteal cells that can proliferate during fracture repair, remodel the new matrix and re-structure it in an organised fashion so that collagen and mineral deposition takes place longitudinally. Lastly, endothelial cells can be grown aligned with the mechanical axis, a major step in building vascularised bone-like constructs.

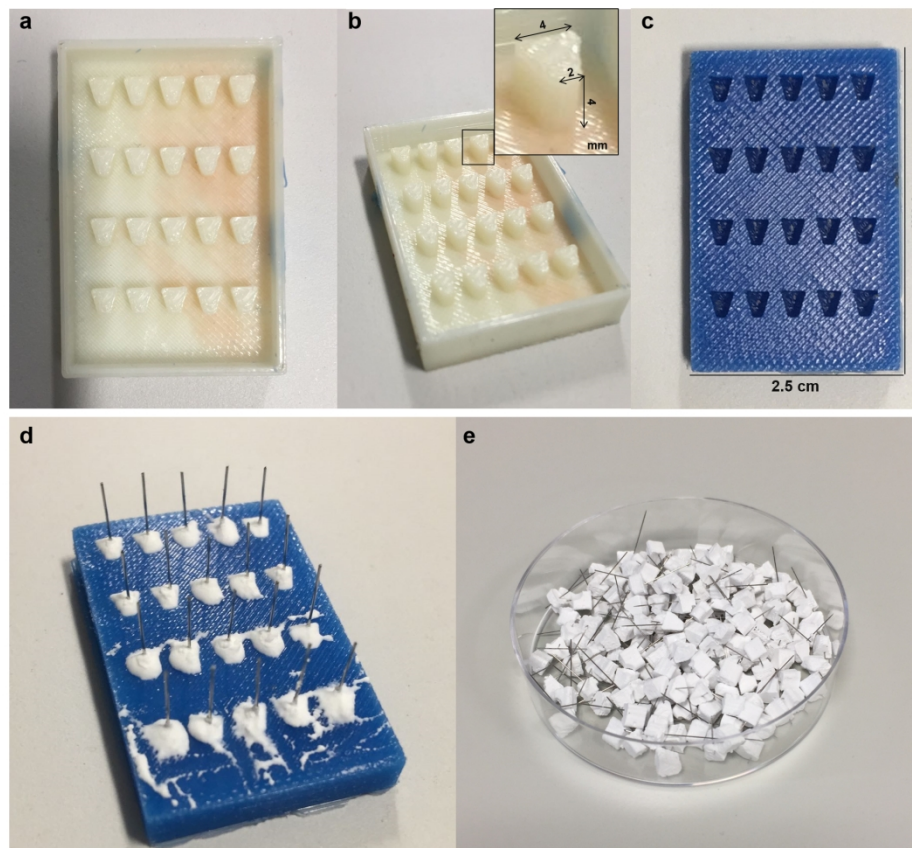


Figure 1. Production of the template and moulds for anchor generation. Rectangular frames containing 4 horizontal rows of 5 trapezoidal shapes each can be printed in plastic using a regular 3D printer (a). These anchors can be up to 4 mm in height and approximately 4 mm x 2 mm in width (b). A standard impression silicone material can be formed on top of this template (c) to generate trapezoidal compartments where individual anchor moulds can be formed (d). The production of several moulds and templates allows the generation of a stock of ceramic anchors in preparation for the study (e).

365x339mm (150 x 150 DPI)

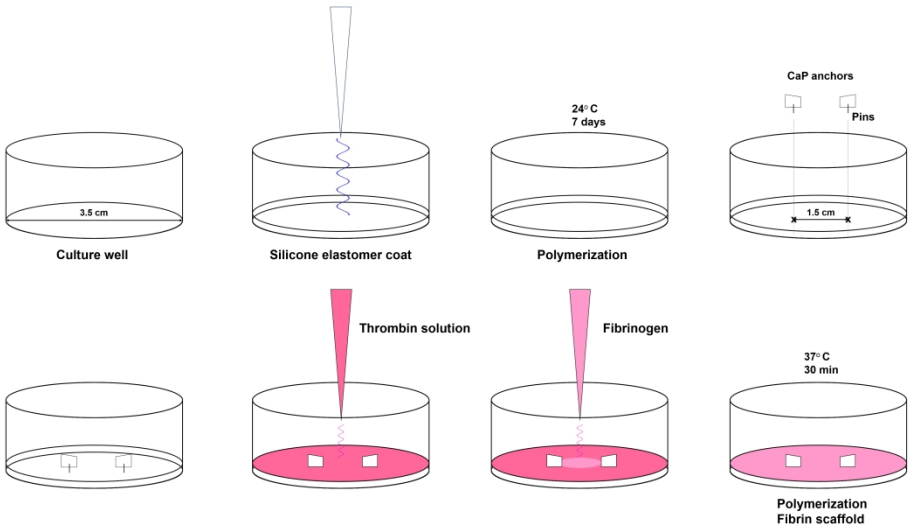


Figure 2. Development of the mineral-fibrin backbone. 35 mm culture wells within 6-well culture dishes are used for developing each construct. Culture wells are coated with 1.5 ml of a silicone elastomer base and are allowed to dry at room temperature for 7 days on a flat surface to allow polymerization. Two anchors are attached to the silicone base using pins inserted during the formation process, at a distance of 1.5 cm from each other. Fibrin scaffolds are produced on the mineral backbone structure through the interaction of the normal plasma components thrombin and fibrinogen. Thrombin is added to a solution containing the cell culture medium and the anti-fibrinolytic agents aminohexanoic acid and aprotinin and 500 μ l are applied to each culture well. Hydrogels are generated by applying 200 μ l of fibrinogen on top of the thrombin solution. Gels are allowed to polymerize for 30 minutes during incubation at 37°C.

777x434mm (150 x 150 DPI)

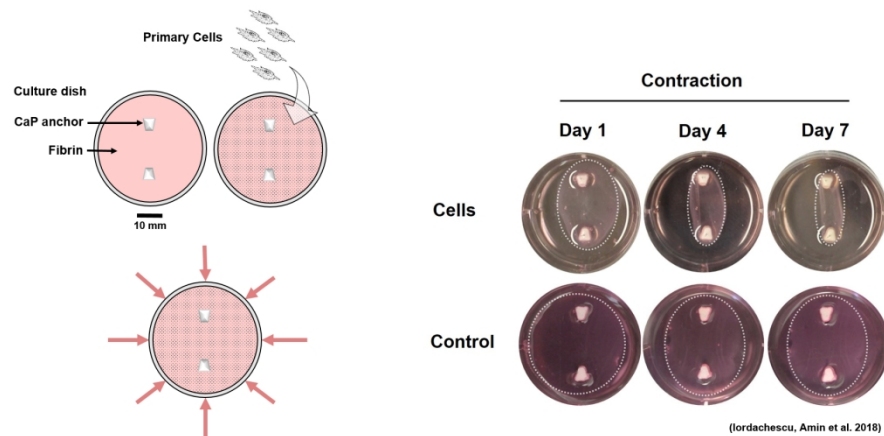


Figure 3. Development of constructs. Primary cells of an osteoprogenitor phenotype are seeded into the fibrin constructs immediately following gel polymerization, at a density of 100K/2ml of cell culture medium (left). The fibrin scaffold is reorganized around the retention points over the first week in culture (right, top panel). Control constructs, developed without cells show a small degree of contraction over 7 days, but remain as flat gels and do not assemble into 3D structures (right, bottom panel). Images are modified from Iordachescu, Amin et al. 2018 and are used under the terms of the Creative Commons Attribution Licence (CC-BY 4.0).

338x180mm (150 x 150 DPI)

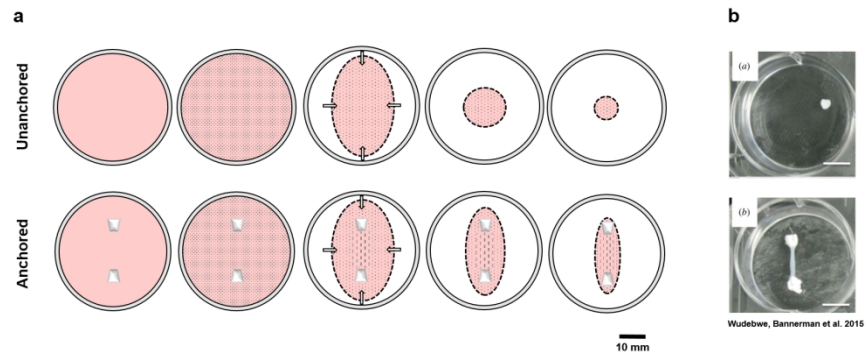


Figure 4. The presence of anchors is required for the formation of longitudinal structures. The two calcium phosphate anchors have a decisive role in matrix contraction and alignment. In the absence of anchors (illustrated in the diagram series in a, top row), cells maximally contract the fibrin scaffolds over three weeks into spherical structures (b, top image), whereas the provision of the 2 retention points (a, bottom row) allows the formation of a cylindrical structure in-between the two calcium phosphate structures (b, bottom image). Scale bars = 10 mm. Images in b are taken from (Wudebwe, Bannerman et al. 2015) and are used under the terms of the Creative Commons Attribution Licence (CC-BY 4.0).

328x153mm (150 x 150 DPI)

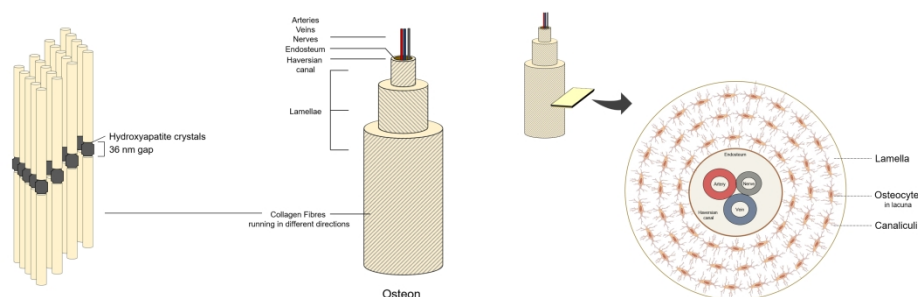


Figure 5. Bone is a highly-organised tissue, from the nano to the macro scale. The image presents a simplified schematic of the organic-inorganic hierarchical structure in lamellar bone tissue. Collagen molecules (normally triple-helical, simplified here) are arranged end-to-end and parallel to each other (left image). These structures contain spaces of approximately 36 nm between them, which facilitate nucleation by apatitic crystals. Mineralised collagenous fibres make up concentric lamellae (middle), each containing collagen fibres orientated in a specific direction. These lamellae form osteons, which act as passageways for blood vessels (arteries and veins) and nerve fibres and are lined internally by the endosteum. Osteocytes, the mature bone cells, are arranged concentrically at the junctions between lamellae (right). They are embedded in lacunae and linked by canaliculi, which allow cell-to-cell communication and connect to the endosteum.

572x233mm (150 x 150 DPI)

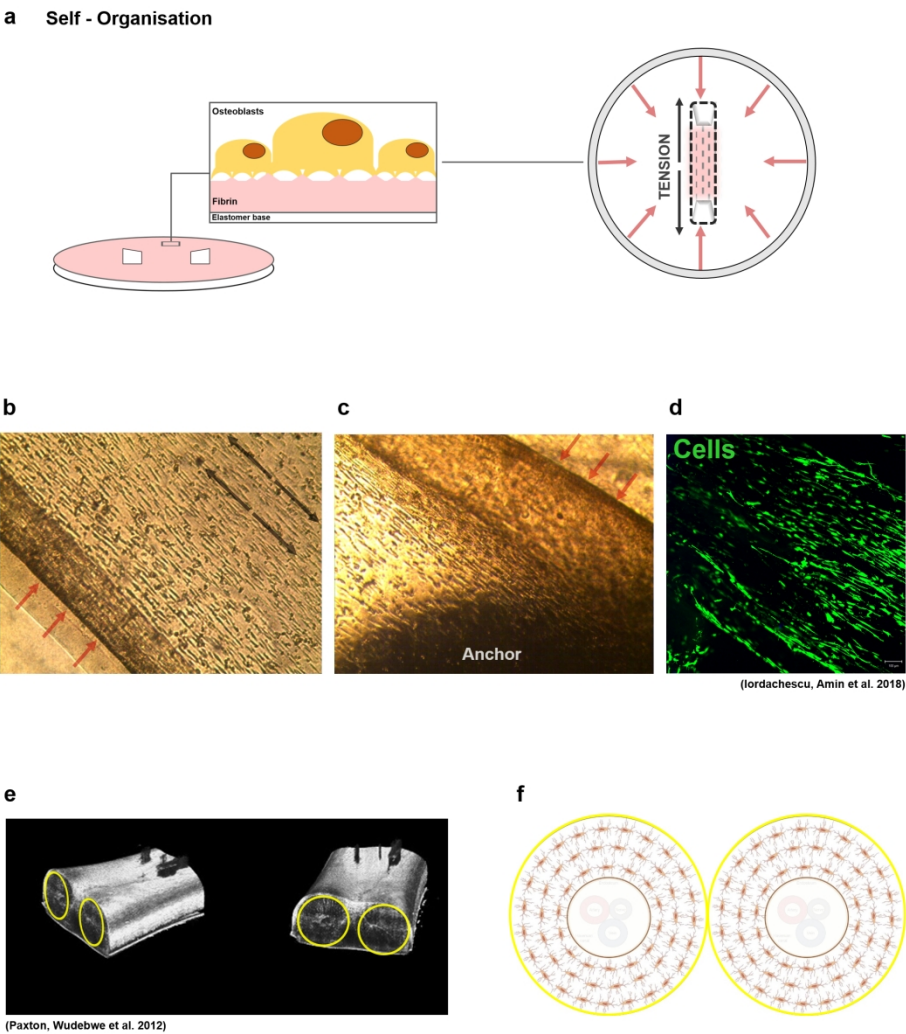


Figure 6. Multi-directional forces lead to self-structuring of constructs. Cells are able to adhere to and remodel the fibrin matrix, creating tensile forces between the two retention points and a spiral-like contraction pattern from the edges of the structures (b, c). Tension leads to cellular alignment along the loading forces (d), which is particularly useful for mimicking the hierarchical cellular organisation and matrix production in bone. Moreover, the longitudinal spiral-like reorganisation of the matrix (e) leads to the creation of basic osteonal-like structures (f), that is particularly useful at later points, when the inserted osteoprogenitor population becomes entrapped inside the highly mineralised matrix, maturing to an osteocytic phenotype (f) and creating canalicular-like structures. Scale bars: d = 100 μ m. Image d is taken from Iordachescu, Amin et al. 2018 and is used under the terms of the Creative Commons Attribution Licence (CC-BY 4.0). Image e is modified from (Paxton, Wudebwe et al. 2012) and is used under the terms of the Creative Commons Attribution Licence (CC-BY).

375x422mm (150 x 150 DPI)

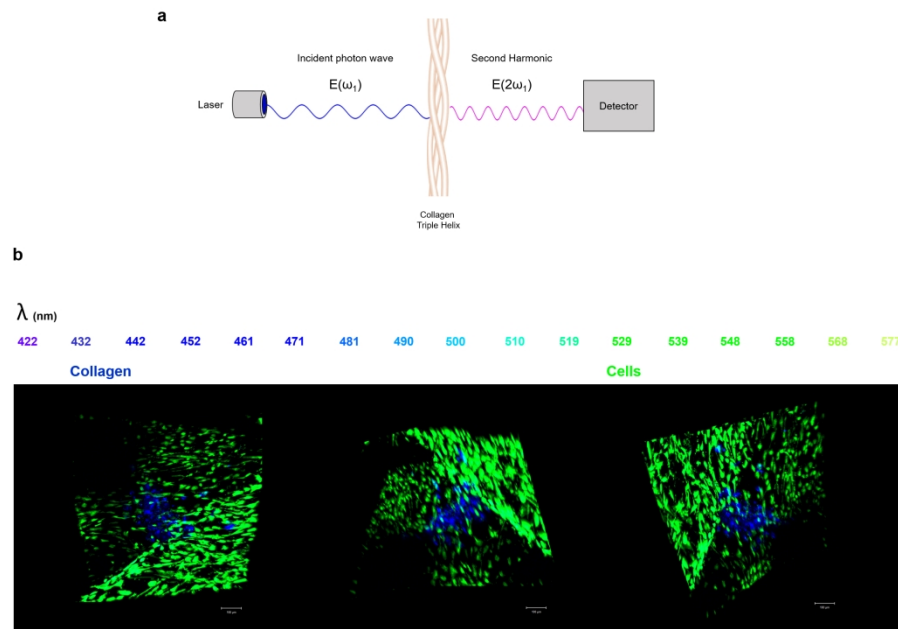


Figure 7. Three dimensional visualisation of collagen deposits and cells in constructs. a, Mature collagen has a triple helical molecular structure which is non-centro-symmetrical. Thus, an incident monochromatic light emitted by a near-infrared laser which interacts with collagen creates an oscillating field at twice the frequency and half the wavelength, an optical effect known as second harmonic generation. b, This non-linear optical effect can therefore be visualised specifically at 432 nm (half the wavelength of the laser) corresponding to the purple-blue area of the spectrum. Cellular structures fluorescently labelled with Calcein AM can be visualised simultaneously in the 481-577 nm region of the spectrum, corresponding to the light blue-green region. The image in b presents different angles of a 3D section acquired from the anchor region of 1 month-old constructs. This technique allows the non-destructive visualisation of the cell-matrix dynamics at the cellular resolution but over the tissue lengthscale, as the tissues are maturing and matrix undergoes ossification. Scale bars = 100 μ m.

483x344mm (150 x 150 DPI)

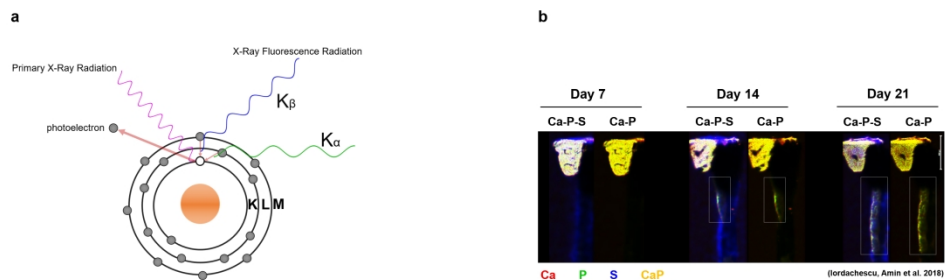


Figure 8. Monitoring mineralisation over time. The initiation and development of mineralisation during the culture period can be monitored non-destructively using X-Ray fluorescence (in this case at the micron resolution), which can detect the presence of chemical elements such as Calcium (Ca) and Phosphorus (P), the main components of the mineral part of bone. a, X-Ray Fluorescence is generated following the ejection of a photoelectron from an atomic shell exposed to high-energy primary X-Ray radiation and the subsequent 'jump' of an outer electron from the near shells in order to fill this vacancy. The process is recorded as X-Ray Fluorescence, with different emission lines for each chemical element and different 'jumps' taking place between different shells (e.g. from the L to the K layer, known as the K_{α} emission line; from M to K, known as K_{β} etc). b, The pattern of localisation of Ca and P can be mapped using this technique and overlaid with that of chemical elements associated with proteins indicative of cellular matrix, such as Sulphur (S). The images in b present micro-XRF maps of live constructs over 21 days, based on Ca, P and S emission lines, which show the progression and co-localisation of Ca and P deposits (combined yellow) from the anchor towards the centre, while the sulphur-rich matrix is represented in blue. Scale bar = 4mm. Image b is taken from Iordachescu, Amin et al. 2018 and is used under the terms of the Creative Commons Attribution Licence (CC-BY 4.0).

533x194mm (150 x 150 DPI)

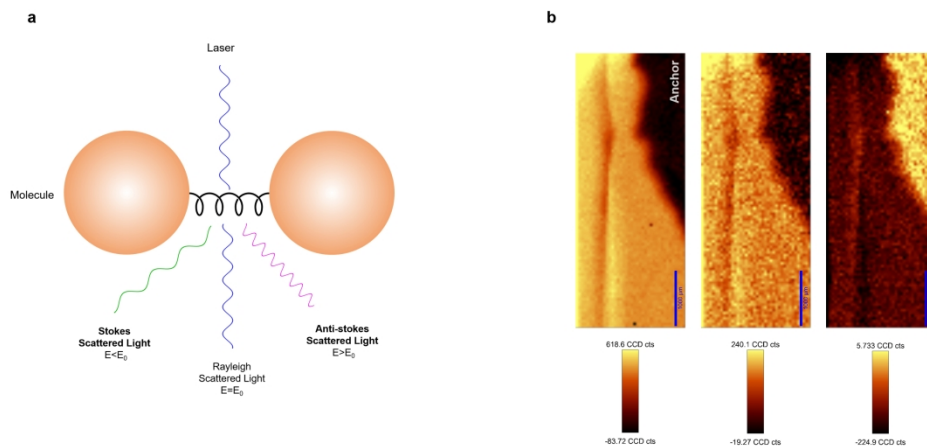


Figure 9. Creating compositional maps of tissues using Raman Spectroscopy. a, Raman spectroscopy relies on the process of inelastic scattering. This technique uses monochromatic light (laser) to excite photons to virtual energy states. When photons are scattered from a molecule most of them are elastically scattered (Rayleigh scattering), having the same energy (frequency and wavelength) as the incident photons. A very small proportion of these photons (1 in 10 million) are scattered inelastically (Raman scattering), which involves the loss (Stokes) or gain (anti-Stokes) of energy due to the interaction of light with vibrations associated with bonds within the sample. Chemical bonds have individual fingerprints that can be used for identification within biological samples and can be locally resolved and co-localised using high-resolution scans (b). Images in b present high-resolution maps of a section of a 7-day old construct, including a fragment of the anchor. These maps are based on the signals from chemical groups present in the organic matrix of constructs, such as phenylalanine (left), amide I present in the newly-forming collagen (middle); as well as the mineral component (tri-calcium phosphate, right) abundant in the anchor region. Scale bars = 1 mm.

522x262mm (150 x 150 DPI)

Long - Term Characterisation

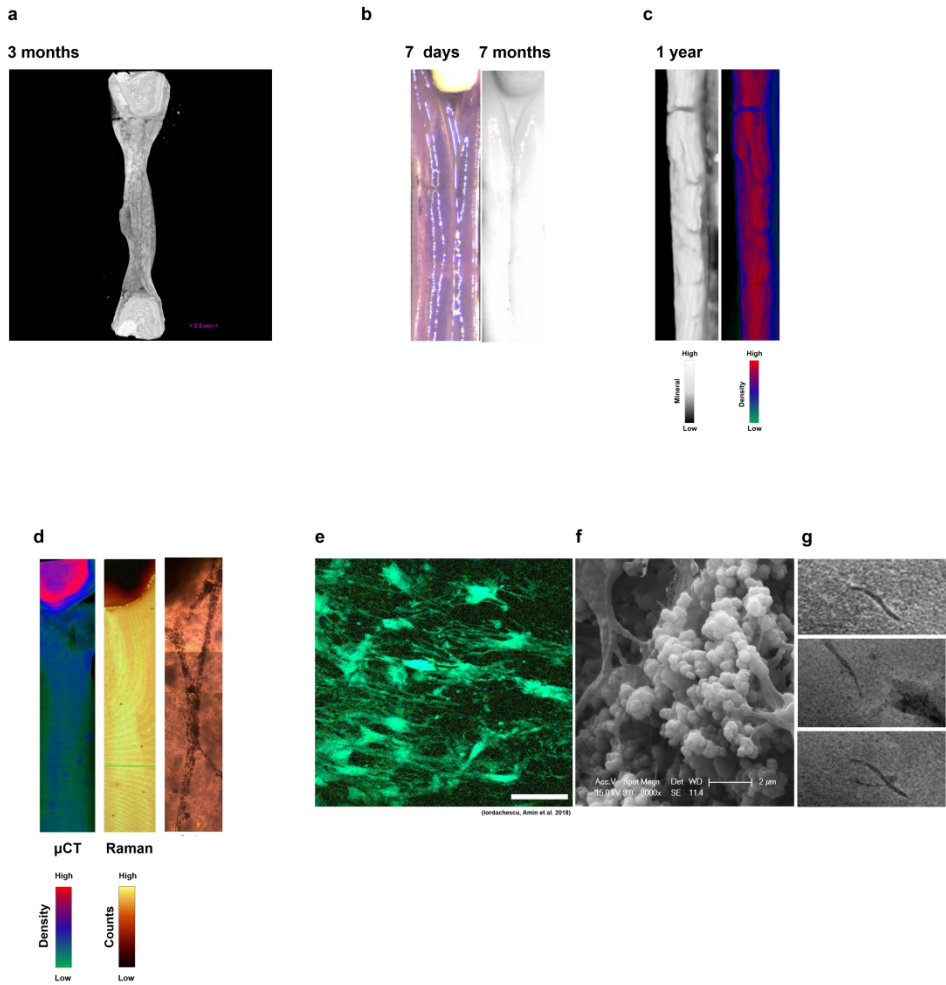


Figure 10. Long term structural evaluation of constructs. Constructs can be grown for periods exceeding 1 year, making them useful for understanding normal and aberrant bone formation. a, As early as 3 months they display a mineral density similar to the calcium phosphate material of the anchor. b, The replacement of the initial matrix with mineralised collagen is visually noticeable, with 7 months-old mature constructs appearing strikingly different from the homogenous initial matrix. The matrix continues to ossify over the following months. Constructs which have been cultured for 1 year show a very dense and compact outer matrix (c). Some of the advantages of this culture system include the ability to monitor ossification longitudinally (d, left), the possibility to characterise these non-destructively in order to monitor the new organic matrix formation (middle, Raman map based on the CH₂ peak of collagen at 1447 cm⁻¹) and the adaptability of the model to include additional populations of cells, including endothelial, which can give rise to a vascularised mature bone system. Another advantage of the system is the ability to differentiate cells to an osteocytic phenotype. Cells can be seen displaying a high number of interconnected projections at 3 months (e) which attach to the highly mineralised matrix (f, SEM image of cellular pods attaching to mineral spheres at 1 year) as well as projecting through it using canalicular (g, top-bottom) and lacunar-like structures (g, middle) (synchrotron Computed Tomography image slices at a resolution of 100 nm). Scale bars: a = 2.5 mm; d = 100 μm. Images c-d are modified from and e is taken from Iordachescu, Amin et al. 2018 and are used under the terms of the Creative Commons Attribution Licence (CC-BY 4.0).

695x755mm (150 x 150 DPI)

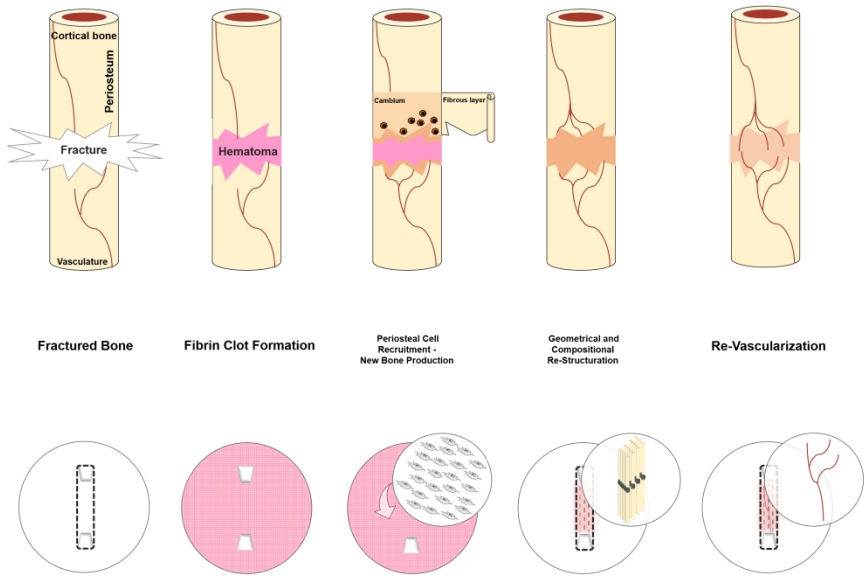


Figure 11. Simulating the fracture-repair process. This model recapitulates several steps of the fracture repair process, including 2 mechanical retention points, a blood clot-like microenvironment, as well as a source of periosteal cells that can proliferate during fracture repair, remodel the new matrix and re-structure it in an organised fashion so that collagen and mineral deposition takes place longitudinally. Lastly, endothelial cells can be grown aligned with the mechanical axis, a major step in buidling vascularised bone-like constructs.

545x378mm (150 x 150 DPI)